Acta Crystallographica Section D
Biological Crystallography
ISSN 0907-4449

Protein crystal structure solution by fast incorporation of negatively and positively charged anomalous scatterers

Ronaldo A. P. Nagem,[a,b] Zbigniew Dauter[c] and Igor Polikarpov[a]*

[a]Laboratório Nacional de Luz Síncrotron, Caixa Postal 6192, CEP 13084-971, Campinas SP, Brazil, [b]Departamento Física, UNICAMP, Caixa Postal 6165, CEP 13084-971, Campinas SP, Brazil, and [c]Synchrotron Radiation Research Section, National Cancer Institute and Brookhaven National Laboratory, Building 725A-X9, Upton, NY 11973, USA

Correspondence e-mail: igor@lnls.br

Received 12 February 2001
Accepted 1 May 2001

The preparation of derivatives by the traditional methods of soaking is one of the most time-consuming steps in protein crystal structure solution by X-ray diffraction techniques. The 'quick cryosoaking' procedure for derivatization with halides (monovalent anions) offers the possibility of significantly speeding up this process [Dauter *et al.* (2000), *Acta Cryst.* D**56**, 232–237]. In the present work, an extension of this technique is proposed and the use of two different classes of compounds (monovalent and polyvalent cations) that can be successfully utilized in the quick cryosoaking procedure for the derivatization and phasing of protein crystals is described. This approach has been tested on hen egg-white lysozyme and has been successfully used to solve the structure of a novel trypsin inhibitor. The possibility of using cations in the fast cryosoaking procedure gives additional flexibility in the process of derivatization and increases the chances of success in phase determination. This method can be applied to high-throughput crystallographic projects.

1. Introduction

The speed of determination of novel macromolecular structures at both in-house and synchrotron X-ray sources is limited to a large extent by the process of preparation of heavy-metal derivatives. The traditional multiple isomorphous replacement (MIR) method (Green *et al.*, 1954; Bragg & Perutz, 1954) for solving protein crystal structures by X-ray diffraction techniques requires several (at least two) isomorphous derivatives. These normally are prepared by introducing different heavy-metal ions into the native crystals. Sometimes, after months of work preparing derivatives, only a few or none at all are useful for determining the crystallographic protein structure. The pace of structure solution could be improved by making use of the anomalous signal in single/multiple isomorphous replacement with anomalous scattering (SIRAS/MIRAS) methods (North, 1965; Matthews, 1966). Single anomalous dispersion (SAD) and multiwavelength anomalous dispersion (MAD; Hendrickson, 1991; Smith, 1991) require only one derivative crystal for crystallographic structure solution, which results in a great reduction in time and effort. In this situation, one can collect only one data set with an optimized anomalous signal or collect only a few data sets using X-rays of different wavelengths. In addition, the most common derivatization procedure applied to MAD includes the use of genetic engineering to replace methionines by selenomethionines in proteins prior to crystallization.

Recently, a new procedure for obtaining derivatives, named 'quick cryosoaking', has been proposed (Dauter *et al.*, 2000). According to this procedure, a quick soak of a protein crystal

Table 1
Details of the preparation and data-collection statistics of HEWL and TRIN crystals.

Statistical values for the highest resolution shells are shown in parentheses. All five derivatives were prepared following the quick cryosoaking procedure for derivatization.

	Nat-HEWL	Cs-HEWL	Gd-HEWL	I-HEWL	Nat-TRIN	Cs-TRIN	I-TRIN
Space group	$P4_32_12$	$P4_32_12$	$P4_32_12$	$P4_32_12$	$P4_32_12$	$P4_32_12$	$P4_32_12$
Unit-cell parameters (Å)	a = 78.58, c = 36.89	a = 78.64, c = 36.79	a = 78.59, c = 36.82	a = 78.62, c = 37.05	a = 58.71, c = 93.75	a = 58.33, c = 93.80	a = 58.42, c = 93.91
Resolution (Å)	21.8–2.00 (2.06–2.00)	18.52–2.30 (2.37–2.30)	18.0–2.30 (2.37–2.30)	21.8–2.30 (2.33–2.30)	25.3–1.83 (1.87–1.83)	22.9–2.00 (2.05–2.00)	25.3–1.92 (1.96–1.92)
No. of observations	105547	150896	152044	147472	123604	312518	285176
No. of unique observations†	7449	9895	9909	9828	15024	20853	23500
$\langle I/\sigma(I)\rangle$	27.3 (19.6)	51.1 (36.6)	35.0 (26.7)	26.3 (17.6)	23.6 (3.3)	33.7 (13.1)	33.7 (13.6)
Multiplicity	14.2 (4.5)	15.2 (14.7)	15.3 (14.3)	15.0 (13.5)	8.2 (5.4)	15.0 (14.7)	12.1 (12.0)
Completeness (%)	99.9 (99.8)	99.8 (100.0)	99.9 (100.0)	98.7 (95.0)	99.7 (97.6)	99.8 (99.5)	99.5 (93.9)
$R_{\rm merge}$‡ (%)	6.6 (7.6)	6.7 (9.1)	8.6 (11.8)	13.0 (16.5)	8.9 (50.8)	9.3 (23.8)	7.3 (17.0)
Data collected (°)	220	360	360	360	130	360	292
Cryoprotectant solution	1.0 *M* NaCl, NaOAc buffer, 15% ethylene glycol	1.0 *M* CsCl, NaOAc buffer, 15% ethylene glycol	0.625 *M* NaCl, 0.250 *M* $GdCl_3$, NaOAc buffer, 15% ethylene glycol	0.75 *M* NaI, NaOAc buffer, 15% ethylene glycol	Mother liquor, 20% ethylene glycol	Mother liquor, 1.0 *M* CsCl, 20% ethylene glycol	Mother liquor, 0.5 *M* NaI, 20% ethylene glycol
Soaking time (s)	60	300	300	60	60	300	180

† Multiplicity of derivative (native) data sets calculated with Friedel-related reflections treated separately (as equivalent). ‡ $R_{\rm merge} = \sum_{hkl} |I - \langle I\rangle| / \sum_{hkl} I$.

in a cryoprotectant solution containing bromide or iodide anions just before freezing the crystal in a cryogenic nitrogen stream leads to incorporation of these anomalous scatterers into the ordered solvent regions around the protein molecules. Halides provide a rapid and convenient way of protein crystal derivatization. Halides are negatively charged ions that bind preferably to positively charged surface areas of the proteins, competing in binding with waters. It was shown that halide derivatization can be successfully used in rapid solution of macromolecular structures (Dauter *et al.*, 2000).

In the current paper, we suggest the extension of the method of rapid cryoderivatization by incorporating short cryosoaks with monovalent cations (such as Cs^+ or Rb^+) and polyvalent cations (such as lanthanides). One might expect that if monovalent cations (Cs^+ or Rb^+) were used instead of anions in the cryoprotectant solution they would preferentially bind to the negatively charged niches on the surface of the macromolecules, which will be distinct from the halide sites. Additional sites, different from those of both monovalent cations and halides, can also be expected if lanthanide ions (Gd^{3+}, Eu^{3+}, Sm^{3+} or Ho^{3+}) are used in the cryoderivatization procedure. Lanthanide ions require a specific coordination sphere for binding and therefore will not compete with monovalent cations and anions in binding to a protein molecule. Since the overall charge and surface-charge distribution of a given protein molecule depends on the pH of the cryoderivatization solution, positively or negatively charged anomalous scatterers might better suit a particular situation.

Different heavy-ion sites permit combined use of these derivatives in MIR(AS) phasing, even when none of them are strong enough to produce interpretable electron-density maps *via* SAD or SIR(AS) methods.

Just for the sake of comparison, an Se atom, one of the most frequently used heavy atoms for SAD/MAD synchrotron data collection, has an anomalous scattering-factor component $\delta f''$ of up to 10 electrons at the white line of the *K* absorption edge (0.98 Å). A Gd atom away from the edge at 1.54 Å has an $\delta f''$ of 12.3 electrons. At the same copper-anode characteristic wavelength (1.54 Å), $\delta f''$ of Cs and I atoms are equal to 7.9 and 6.8 electrons, respectively, as estimated by the program *CROSSEC* (Cromer, 1983). This opens the way to using the fast cryoderivatization procedure combined with relatively long wavelength data collection (1.5–1.6 Å), which can be performed far from the absorption edges of the anomalous scatterers at the synchrotron (including medium-energy machines) as well as rotating-anode X-ray sources.

In the present work, we describe the use of the quick cryosoaking procedure with positively and negatively charged anomalous scatterers to phase hen egg-white lysozyme (HEWL) and a novel trypsin inhibitor (TRIN). Caesium chloride and gadolinium (III) chloride were used in the cryoprotectant solution as a source of positively charged anomalous scatterers and sodium iodide as a source of negatively charged anomalous scatterers. Diffraction data were collected at the Brazilian National Synchrotron Light Laboratory, a medium-energy synchrotron ring, using X-rays with the wavelength 1.54 Å.

2. Materials and data acquisition

HEWL (Sigma) was crystallized following standard protocols (hanging drops) at 291 K. The crystallization solution consisted of 20–30 mg ml^{-1} protein, 0.5 *M* NaCl in 0.025 *M* sodium acetate buffer pH 4.5 and the well solution was 1.0 *M* NaCl in 0.050 *M* sodium acetate buffer.

A novel trypsin inhibitor has been extracted from the seeds of *Copaifera langsdorffi* (also known as Copaíba), a tree which is widespread in the central region of Brazil. The inhibitor has a molecular weight of 18 kDa. It was purified to homogeneity using ammonium sulfate precipitation followed by anion-exchange and affinity chromatography. The hanging-drop method performed at pH 4.8 with PEG 8000 as a precipitant was used to obtain well diffracting crystals of TRIN (work to be published).

Sodium iodide, caesium chloride and gadolinium (III) chloride used in the quick cryosoaking derivatization procedure were of analytical grade and were purchased from Sigma and Hampton Research Corp.

Native and derivative data sets for both proteins were collected at the Protein Crystallography beamline (Polikarpov, Oliva *et al.*, 1997; Polikarpov, Perles *et al.*, 1997) at the Brazilian National Synchrotron Light Laboratory (Campinas, SP, Brazil) using a MAR345 image plate.

X-ray diffraction images were integrated with *DENZO* (Otwinowski & Minor, 1997) in *P*1 to allow a better fit of predicted spots and measured reflections. *SCALEPACK* (Otwinowski & Minor, 1997) was used to scale images in the correct space group.

The diffraction data were collected with a high multiplicity resulting from the wide total angular range of rotation (130–360°) and the high symmetry of the crystals. No attempts were made to measure Bijvoet-related reflections close in time or on the same rotation image.

For all derivatives, a single crystal was transferred for a short period of time (60–300 s) to a cryoprotectant solution containing heavy-atom compounds (NaI, CsCl or $GdCl_3$) at different concentrations (0.25–1.0 *M*) and then quickly frozen in a fibre loop in a nitrogen-gas stream at 100 K. The synchrotron-radiation wavelength was set to 1.54 Å. Details of the preparation of the native crystals and derivatives for data acquisition as well as data-collection statistics are given in Table 1. In order to simulate a typical X-ray diffraction experiment, native and derivative HEWL data sets were only collected to 2.0 and 2.3 Å resolution, respectively.

The quality of each data set and the presence of the anomalous signals of Cs, I and Gd atoms were controlled following the $|\Delta F|/F$ and $|\Delta F|/\sigma(\Delta F)$ ratios as a function of resolution for each derivative. The results are summarized in Fig. 1.

3. Results and discussion

3.1. The heavy-atom substructures

The use of anomalous difference Patterson maps to locate heavy-atom sites was successfully employed for the Gd-HEWL derivative. In all other cases direct methods were used.

Scaled intensities for each derivative were submitted to *SnB* 2.1 (Weeks & Miller, 1999), where normalized anomalous differences (diff*E*) were calculated with the program *DREAR* (Blessing & Smith, 1999). Normalized anomalous differences were then used by *SnB* to find the relative positions of the caesium, iodide and gadolinium ions for HEWL derivatives and the caesium and iodide ions for TRIN derivatives.

The location of major heavy-atom sites by direct methods was a straightforward task when all data collected were included in a search. Default parameters suggested by *SnB* were used in most of the cases. In some cases increases in the number of reflections, triple invariants and *SnB* cycles were necessary to successfully find heavy-atom substructure within the equivalent sets of possible origin shifts or enantiomers.

In the case of TRIN, the caesium-derivative data set was used in the heavy-atom search. A total of 500 diff*E* values (Blessing & Smith, 1999) were used to generate 5000 triple invariants. Four random atom positions were generated for each of 1000 trial structures and each trial structure was subjected to 30 *SnB* cycles, each cycle consisting of phase refinement and Fourier filtering. The bimodal distribution of the $R_{\rm min}$ histogram was used to identify the correct solution (Debaerdemaeker & Woolfson, 1983; Hauptman, 1991; De

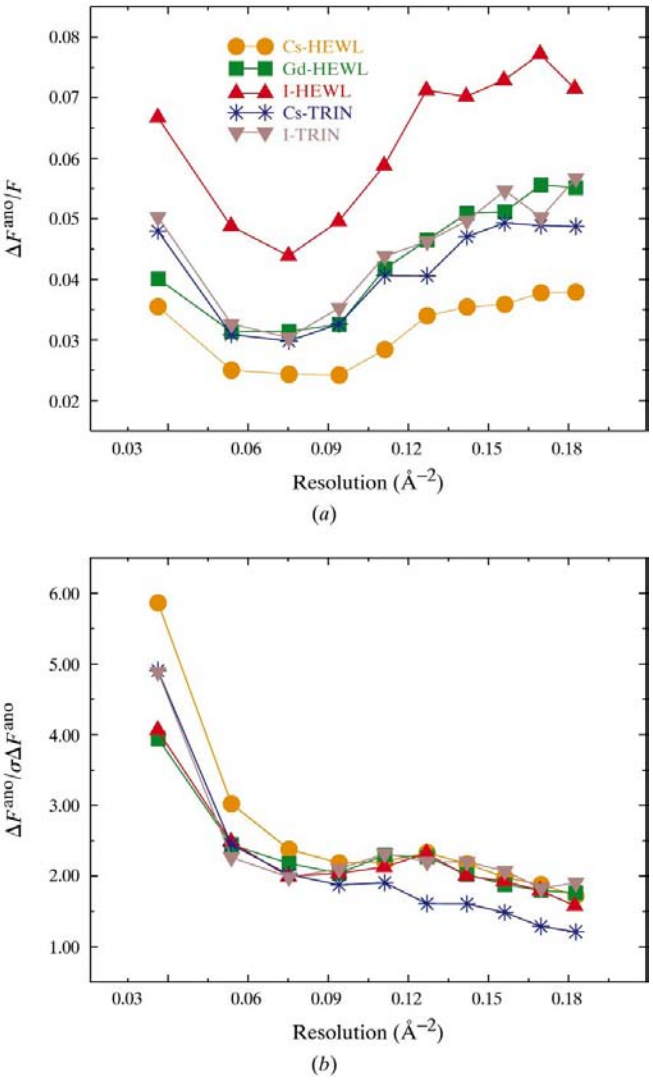

Figure 1
Statistics of the anomalous signal in derivative data sets. (*a*) $|\Delta F|/F$; (*b*) $|\Delta F|/\sigma(\Delta F)$ as a function of resolution. All derivatives were prepared according to the quick cryosoaking procedure for derivatization.

Titta *et al.*, 1994). The relative positions of iodide anions were then located in cross-phased Fourier maps in respect to the origin of caesium sites using the *CNS* package (Brunger *et al.*, 1998).

3.2. Phasing

For all derivatives, the heavy-atom substructure obtained directly from *SnB* was initially refined with the *CNS* package using anomalous and isomorphous difference Fourier maps. Refined coordinates were then input into *SHARP* (de La Fortelle & Bricogne, 1997) and different methods (SAD, SIRAS and MIRAS) were used for phase calculation. Density modification with solvent flattening was then performed using the program *SOLOMON* (Abrahams & Leslie, 1996).

Independently, to check the correctness of heavy-ion positions, a lysozyme model (PDB code 1lz8) was refined in *CNS* and *SHELXL* (Sheldrick & Schneider, 1997) against each HEWL data set. The resulting *R*-factor values were in the range 18–19% and $R_{\rm free}$ values were in the range 19–22%. The heavy-atom positions released by *SnB* and refined in *CNS* could then be checked using anomalous difference Fourier maps ($\Delta F^{\rm ano}$, $\varphi_{\rm calc} - 90^\circ$). Cs-HEWL and I-HEWL anomalous difference Fourier maps showed a number of anomalous peaks surrounding the protein surface. On the other hand, only three major sites were confirmed by the Gd-HEWL anomalous map. The superposition of all three anomalous difference Fourier maps and the ion distribution around the HEWL electrostatic surface are shown in Figs. 2(*a*) and 2(*b*), respectively. The figures of merit and a correlation of the electron-density maps obtained by SAD, SIRAS and MIRAS methods to the refined maps ($2mF_{\rm obs} - DF_{\rm calc}$,$\varphi_{\rm calc}$) for HEWL and TRIN are given in Table 2.

The SIRAS phases obtained with the positions of five caesium cations in the Cs-TRIN derivative were used to find six iodide anions in the second derivative. A MIRAS electron-density map was calculated with *SHARP*/*SOLOMON*. A representative part of the map is shown in Fig. 3(*a*). All 11 heavy-atom sites were included in the phasing procedure. Based on this map, we used the program *ARP*/*wARP* (Perrakis *et al.*, 1999) in mode '*warpNtrace*' to build a hybrid model of TRIN. A specific region of the output *wARP* electron-density map and with the built hybrid model is shown in Fig. 3(*b*).

A total of 20 automatic building cycles were performed in *wARP*. In the last cycle, up to 92% of the structure was traced in six chains. Evolution of model building and quality of the model can be followed in Fig. 4. The number of traced residues and the *R* factor for the hybrid model as a function of automatic building cycles is shown.

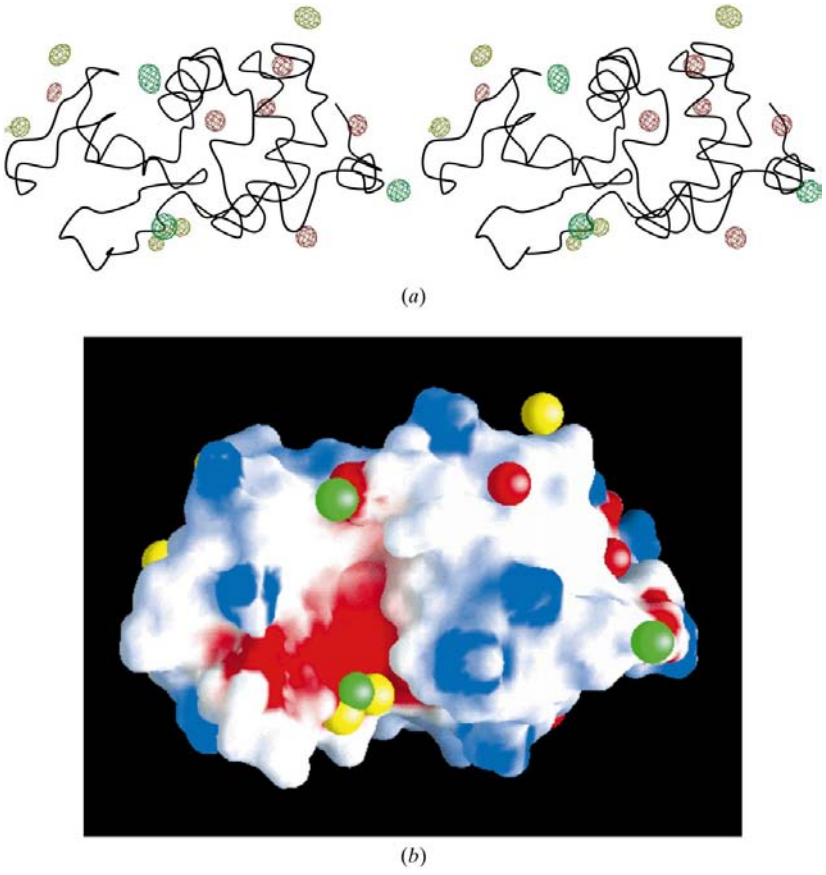

Figure 2
(*a*) Stereoview of a coil representation of HEWL and anomalous difference Fourier maps of Cs, Gd and I derivatives prepared by the quick cryosoaking procedure, shown in yellow, green and red, respectively. The three maps are contoured at the 10σ level. The figures were prepared using *MOLSCRIPT* (Kraulis, 1991), *Bobscript* (Esnouf, 1997) and *Raster3D* (Merritt & Bacon, 1997). (*b*) Distribution of ions around HEWL electrostatic surface as calculated by *GRASP* (Nicholls *et al.*, 1991). Diffusion of ions into protein crystal channels is relatively fast. Even within a short period of time (a few seconds), anions (or cations) preferentially bind positively (or negatively) charged patches of the macromolecule surface. Caesium, gadolinium and iodide ions are represented as yellow, green and red spheres, respectively. Both figures are in the same orientation.

3.3. Environment of anomalous sites

As can be seen from Fig. 2, gadolinium and caesium cations bind in negatively charged niches at the protein surface, interacting mostly with glutamic and aspartic acid side chains, waters and main-chain carbonyl groups. On the other hand, iodide anions are normally located in other surface areas, preferentially bound to lysine and arginine. For a detailed description of the environment of iodide (halide) anions see Dauter *et al.* (2000). The binding sites are distinct and particular for all three HEWL derivatives.

Caesium cations, similar to iodide anions, are distributed around the protein surface of HEWL. A comparison of the native and caesium-derivative electron-density maps show that caesium cations indeed replace coordinated water molecules, leading to elliptical electron-density patterns where caesium and waters share sites that are close to each other. The five

Table 2
Relevant parameters of electron-density maps obtained by SAD, SIRAS and MIRAS methods using HEWL and TRIN derivatives prepared by the quick cryosoaking procedure.

Phasing method	Data sets used in phasing	Resolution range	FOM before *SOLOMON*	FOM after *SOLOMON*	Correlation†
SAD	I-HEWL	18.00–2.30	0.48	0.91	0.62
SIRAS	Nat/Gd-HEWL	18.00–2.30	0.31	0.96	0.71
SIRAS	Nat/I-HEWL	18.00–2.30	0.62	0.95	0.81
MIRAS	Nat/Cs/Gd-HEWL	18.00–2.30	0.45	0.95	0.64
MIRAS	Nat/Cs/I-HEWL	18.00–2.30	0.63	0.95	0.79
MIRAS	Nat/Cs/Gd/I-HEWL	18.00–2.30	0.75	0.95	0.85
SAD	I-TRIN	22.90–2.00	0.39	0.93	0.54
SIRAS	Nat/Cs-TRIN	22.90–2.00	0.48	0.95	0.51
SIRAS	Nat/I-TRIN	22.90–2.00	0.53	0.96	0.74
MIRAS	Nat/Cs/I-TRIN	22.90–2.00	0.63	0.97	0.84

† Correlation coefficients of TRIN maps were calculated using a reference electron-density map ($2mF_{obs} - DF_{calc}, \varphi_{calc}$) obtained on the basis of current structure built and refined by *wARP* (Perrakis *et al.*, 1999). The structure is more than 92% complete.

prominent caesium sites were found between 2.7 and 3.7 Å from main-chain carbonyl groups, from the negatively charged side chains of aspartate and glutamate residues and from the polar side chains of asparagine and serine residues. A typical example of a caesium site is illustrated in Fig. 5(*a*).

Gadolinium cations require a coordination sphere and are therefore more specific in binding compared with caesium cations and iodide anions. Nevertheless, gadolinium cations are able to bind to negatively charged and polar residues on the surface of HEWL (and other proteins) even in quick cryosoaking experiments. Fig. 5(*b*) shows the major gadolinium site. It is coordinated by six nearest neighbours: the carboxyl group of Asp52 (at a distance of 1.8 Å) and five waters (2.4, 2.6, 2.7, 2.7 and 2.8 Å from the Gd atom).

All other gadolinium cations are found inside channels between symmetry-related proteins or close to O atoms in asparagine and aspartate side chains. Several water molecules take part in the coordination sphere.

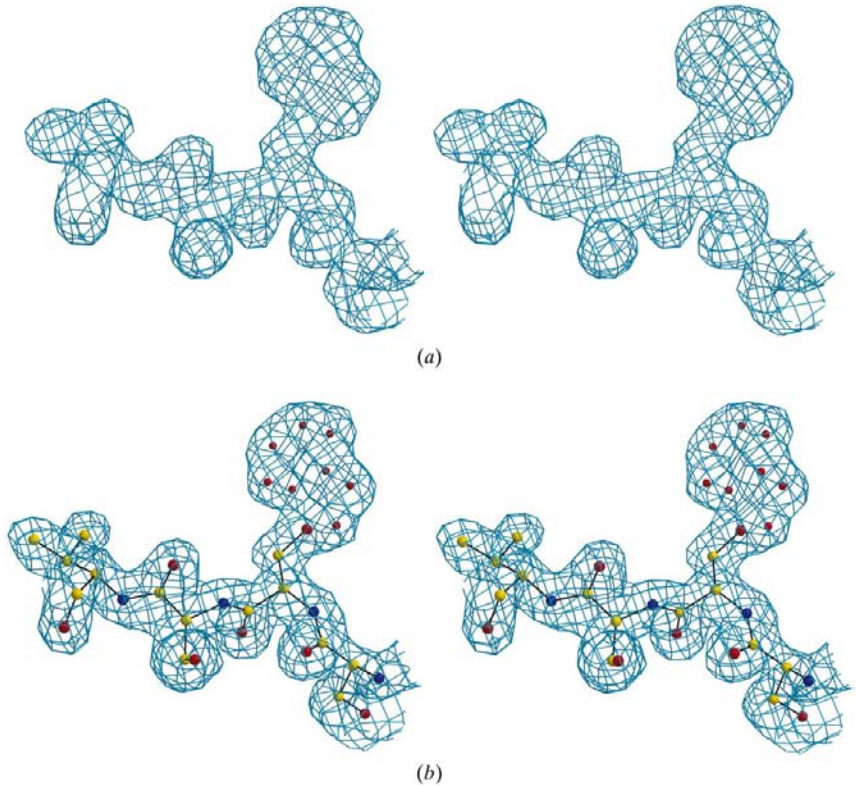

Figure 3
(*a*) Stereoview of a representative part of the TRIN electron-density map after density modification performed by *SOLOMON*. The solvent-flattened electron-density map was used as an input to *wARP* for automatic model building. (*b*) A part of a hybrid model of TRIN built by *wARP* in a ($2mF_{obs} - DF_{calc}, \varphi_{calc}$) electron-density map. Inserted waters (small red spheres) clearly define a tryptophan side chain.

4. Conclusions

In the present work, we show that the monovalent and polyvalent cations Cs^+ and Gd^{3+} can be successfully used in the quick cryosoaking procedure for derivatization and phasing of protein crystals. Caesium cations as well as monovalent anions seem to be less destructive to protein crystals. Their concentration in the cryoprotectant solution can be increased to 1.0 *M* or even higher without significant deterioration of the protein crystal diffraction quality. On the other hand, the use of lanthanides requires more care. Their concentration in the cryoprotectant solution must be correctly chosen to avoid crystal degradation. Nevertheless, lower concentrations of lanthanides (0.25 *M*; about 100 times higher than the concentration of the heavy metal in traditional soaks) associated with a slightly longer time of soaking (up to 300 s) seem to be effective.

The addition of cations to the quick cryosoaking derivatization procedure opens up the possibility of fast and rational searching for derivatives. For a particular protein, its pI and the pH range of the crystallization solution are normally fixed and therefore cations and/or anions may be chosen to best suit the derivatization experiment. The residues most frequently involved in binding of the anomalous scatterers in quick cryosoaking experiments with monovalent anions are lysine, arginine and histidine (positively charged side chains) and with monovalent cations are aspartate and glutamate (negatively charged side chains). It should be

emphasized that at lower pHs and for basic proteins, halides may be particularly suitable for quick cryosoaking procedures. On the other hand, at alkaline pHs and for proteins with high contents of glutamic and aspartic acid residues, positively charged anomalous scatterers may be more suitable for quick cryoderivatization.

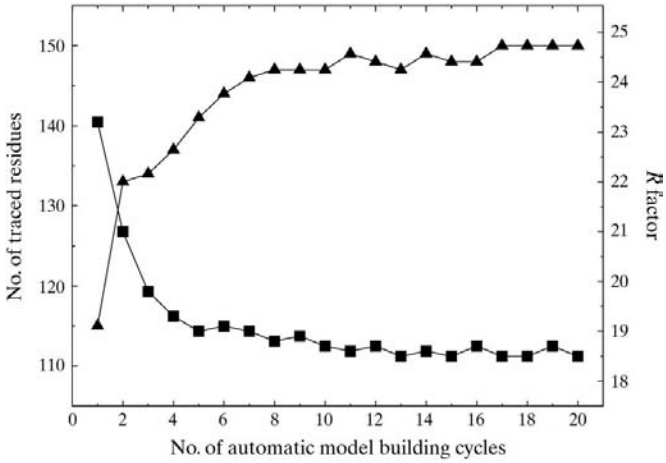

Figure 4
Number of traced residues and the crystallographic *R* factor as a function of *warpNtrace* cycles on the example of TRIN. In the last cycle 150 residues were traced in six chains. More than 92% of the structure were correctly built.

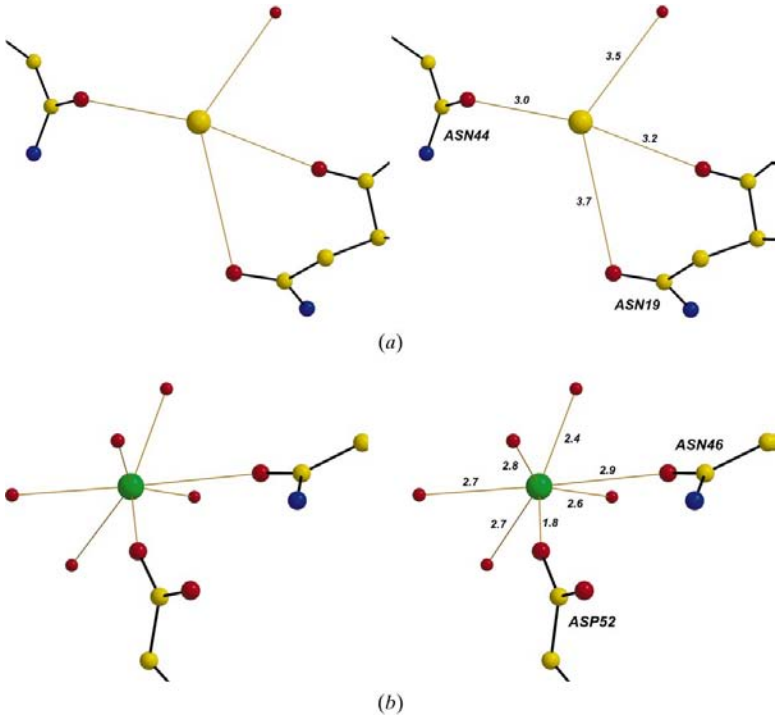

Figure 5
Stereoview of the caesium- and gadolinium-binding sites in HEWL derivatives prepared by quick cryosoaking. (*a*) A caesium cation (yellow sphere) relatively close to the O atoms (red spheres) of the Asn44 and Asn19 side chains, a carbonyl group and a water molecule. (*b*) The major gadolinium site (green sphere) is coordinated by six neighbouring atoms: Asp52 carboxyl group (at a distance of 1.8 Å) and five water molecules (at a distances of 2.4, 2.6, 2.7, 2.7 and 2.8 Å).

The absorption edges of caesium and iodide ions lie beyond the easily accessible wavelength range for typical diffraction experiments. However, even at the wavelength of 1.54 Å, caesium, iodine and gadolinium have a significant anomalous signal which can be utilized in the SAD or SIRAS/MIRAS methods. Since copper-anode X-ray sources can be used in such experiments, it may very well be possible for experimenters to validate their quick cryosoaked derivatives prior to synchrotron visits.

Synchrotron radiation can be used to increase the anomalous effect in gadolinium derivatives since its *L* absorption edge can be easily reached at standard beamlines. Besides, Rb (rubidium) can be used in place of caesium cations in the same way as bromine was used instead of iodine in MAD experiments (Dauter *et al.*, 2000). At the dedicated MAD beamlines of high-energy synchrotron X-ray sources, the *K* absorption edge of rubidium (0.82 Å) can easily be reached (A. Joachimiak, personal communication). Although the anomalous scattering factors of atoms which can potentially be used for quick cryosoaking derivatization procedure are comparable or even higher than those of common Se-Met derivatives, the occupancies of quick cryosoaked ions are generally less than unity (normally close to 0.7–0.5). Therefore, the ultimate molecular weight of the protein that can be solved using quick cryosoaking procedure needs further experimental studies.

The quick cryosoaking approach with halides and cations requires little preparative effort and may be particularly applicable for high-throughput crystallographic projects. Novel proteins that require rapid three-dimensional structure elucidation and diffract beyond 2.0 Å resolution are potential targets for these approach. The high-resolution data increase the chances of an automatic building of the three-dimensional model resulting in a structure solution within the shortest period of time.

The authors are grateful to J. R. Brandão Neto for help with data collection and Valeria Forrer and Renata Carmona e Ferreira for help with crystallization of the proteins. Financial help from CNPq and FAPESP *via* grants 99/03387-4 and 98/06218-6 is acknowledged.

References

Abrahams, J. P. & Leslie, A. G. W. (1996). *Acta Cryst.* D**52**, 30–42.
Blessing, R. H. & Smith, G. D. (1999). *J. Appl. Cryst.* **32**, 664–670.
Bragg, W. L. & Perutz, M. F. (1954). *Proc. R. Soc. London Ser. A*, **225**, 315.
Brunger, A. T., Adams, P. D., Clore, G. M., DeLano, W. L., Gros, P., Grosse-Kunstleve, R. W., Jiang, J.-S., Kuszewski, J., Nilges, M., Pannu, N. S., Read, R. J., Rice, L. M., Simonson, T. & Warren, G. L. (1998). *Acta Cryst.* D**54**, 905–921.
Cromer, D. T. (1983). *J. Appl. Cryst.* **16**, 437–438.
Dauter, Z., Dauter, M. & Rajashankar, K. R. (2000). *Acta Cryst.* D**56**, 232–237.

Debaerdemaeker, T. & Woolfson, M. M. (1983). *Acta Cryst.* A**39**, 193–196.
De Titta, G. T., Weeks, C. M., Thuman, P., Miller, R. & Hauptman, H. A. (1994). *Acta Cryst.* A**50**, 203–210.
Esnouf, R. M. (1997). *J. Mol. Graph.* **15**, 133–138.
Green, D. W., Ingram, V. M. & Perutz, M. F. (1954). *Proc. R. Soc. London Ser. A*, **225**, 287.
Hauptman, H. A. (1991). *Crystallographic Computing 5: from Chemistry to Biology*, edited by D. Moras, A. D. Podjarny & J. C. Thierry, pp. 324–332. Oxford: IUCr/Oxford University Press.
Hendrickson, W. A. (1991). *Science*, **254**, 51–58.
Kraulis, P. (1991). *J. Appl. Cryst.* **24**, 946–950.
La Fortelle, E. de & Bricogne, G. (1997). *Methods Enzymol.* **276**, 472–494.
Matthews, B. W. (1966). *Acta Cryst.* **20**, 82–86.
Merritt, E. A. & Bacon, D. J. (1997). *Methods Enzymol.* **277**, 505–524.
Nicholls, A., Sharp, K. A. & Honig, B. (1991). *Proteins: Struct. Funct. Genet.* **11**, 281–296.
North, A. C. T. (1965). *Acta Cryst.* **18**, 212–216.
Otwinowski, Z. & Minor, M. (1997). *Methods Enzymol.* **276**, 307–326.
Perrakis, A., Morris, R. J. & Lamzin, V. S. (1999). *Nature Struct. Biol.* **6**, 458–463.
Polikarpov, I., Oliva, G., Castellano, E. E., Garratt, R., Arruda, P., Leite, A. & Craievich, A. (1997). *Nucl. Instrum. Methods A*, **405**, 159–164.
Polikarpov, I., Perles, L. A., de Oliveira, R. T., Oliva, G., Castellano, E. E., Garratt, R. & Craievich, A. (1997). *J. Synchrotron Rad.* **5**, 72–76.
Sheldrick, G. M. & Schneider, T. R. (1997). *Methods Enzymol.* **277**, 319–343.
Smith, J. L. (1991). *Curr. Opin. Struct. Biol.* **1**, 1002–1011.
Weeks, C. M. & Miller, R. (1999). *J. Appl. Cryst.* **32**, 120–124.